Hindawi
Complexity
Volume 2021, Article ID 6623485, 16 pages
https://doi.org/10.1155/2021/6623485

Research Article

Study on an Intelligent Prediction Method of Ticket Price in a Subway System with Public-Private Partnership

Shengmin Wang,[1,2] **Jun Fang**,[1] **Lanjun Liu**,[1] **and Han Wu**[1]

[1]*School of Civil Engineering and Architecture, Wuhan University of Technology, Wuhan 430070, China*
[2]*School of Safety Science and Emergency Management, Wuhan University of Technology, Wuhan 430070, China*

Correspondence should be addressed to Han Wu; wuhan20170620@163.com

Received 22 December 2020; Revised 4 July 2021; Accepted 19 July 2021; Published 27 July 2021

Academic Editor: Haitham Afan

The accurate and rapid prediction of ticket prices for a public-private partnership (PPP) subway system, which is an important research topic in the field of civil engineering management, is of critical importance to ensure its smooth operation. To effectively cope with the effects of multiple influencing factors and strong nonlinearity among them, the mean impact value (MIV) method and the back-propagation (BP) feed-forward neural network improved by the sparrow search algorithm (SSA) are used in this study to develop an intelligent prediction model. First, we considered the relationship of the supply and the subway system service, which is a typical quasi-public product, and analyzed the relevant factors affecting its price adjustment. Then, we developed an intelligent method for the prediction of ticket prices based on the SSA-BP. This model not only makes full use of the powerful nonlinear modeling ability of the BP algorithm, but also takes advantage of the strong optimization ability and fast convergence speed of the SSA. Finally, this study screened out the key input factors by adopting the MIV method to simplify the structure of the BP algorithm and achieve a high prediction accuracy. In this study, Beijing Subway Line 4, Wuhan Metro Line 2, and Chengdu Metro Line 1 were selected as case study sites. The results showed that the linear correlations between influencing factors and ticket price for the PPP subway system service were weak, which indicated the need for using nonlinear analysis methods such as the BP algorithm. Compared with other prediction methods (the price adjustment method based on PPP contract, the traditional BP algorithm, the BP neural network improved by the genetic algorithm, the BP algorithm improved by the particle swarm optimization, and the support vector machine), the model proposed in this paper showed better prediction accuracy and calculation stability.

1. Introduction

Currently, numerous subway systems are being built around the world to meet the needs of rapid urban development [1]. As an important infrastructure, a subway system has the characteristics of large initial investment, high operating cost, and long payback period, which drive decision-makers to often use the public-private partnership (PPP) to build subway systems [2, 3]. Under the PPP mode, the private sector cooperates with the government to participate in the construction and operation of subway systems. The private sector is mainly responsible for the financing, construction, operation, and maintenance of subway systems. Government departments mainly provide policy support, land, and operating subsidies. For the government, the goal is the construction of a subway system that is compatible with the sustainable development of the country, and the charging price for the subway system service needs to maintain its public welfare attribute. For the private sector, investing in the construction of PPP subway system projects can generate considerable investment income during the operation period. For the public (customers), the charging price for the subway system service needs to meet their ability to pay. If the price is too high, it will be unbearable for the customers, which will lead them to choose other means of transport for competitive services. If the price is too low, the return on the private sector investment will not be sufficient to grow their assets. Therefore, predicting the ticket price rapidly and accurately is of critical importance to ensure an acceptable return on the funds invested by the private sector and the welfare level of the public, which decide whether the subway system could be implemented smoothly.

At present, subway systems mainly adopt either a single fare system or a mileage-based pricing system, of which the latter is the most common, and this is adopted by this study. The ticket price in this study is the price per kilometre and is also the price for the cooperation game between the government agencies and the private sector during the operation period of the PPP subway system. If the traditional financial calculation method is adopted, the ticket price studied in this paper is the ticket price per kilometre in order to achieve the predetermined revenue target. With this price, which is the research object of this paper, the subway operating company is able to further put forward the actual selling price for the public. In addition, the determination of the final price for the customer is a more complicated issue, which is not the content of this paper.

In terms of research objects, relevant scholars have conducted some research on the PPP subway systems, but the related research results mainly focused on the concept of PPP, risk sharing, performance management, and driving force [4]. Chang [5] analyzed the driving force and feasibility of adopting the PPP mode in Beijing Metro Line 4 (Beijing, China). Sturup [6] took Copenhagen's Metro System (Copenhagen, Denmark) and Melbourne City Link (Melbourne, Australia) as examples and analyzed the problems that might arise in the implementation of the PPP subway system projects. Gordon et al. [7] studied the performance management of the PPP subway system in the Sydney Metro (Sydney, Australia). Li and Love [8] evaluated the impact of land appreciation on the economic feasibility of the Delhi Airport Metro Express Line (New Delhi, India). Cohen and Boast [9] studied the game between social capital and government of Milan Metro Line 4 (Milan, Italy). However, it was not difficult to find that most of this research was focused on the field of public administration or sociology, and there was almost no research on the operation and management contents, such as price prediction of PPP subway systems. The main reasons for this situation might be as follows: (1) The research on PPP subway systems is still at a theoretical stage, and the pertaining research has not yet reached the stage of operation management. (2) The PPP subway system is too complicated, which requires a lot of effort and time to obtain enough engineering data to support the related research on price adjustment.

In terms of research methods, the PPP subway system has many participants, many years of operation, and complex management; as a result, there are many factors that affect the price of PPP subway system service [10]. Therefore, in engineering practice and scientific research, there is no universal and unified PPP subway system service price adjustment or prediction mechanism. Currently, in the practice of the PPP subway system management, the price of the subway ticket is often adjusted according to the price adjustment conditions agreed on in the PPP contract. This method has the disadvantages of slow prediction speed and unstable prediction results, which easily leads to the instability of the subway operating income and ultimately results in bad consequences, such as the failure of the PPP subway system cooperation [11]. In addition, the multiple regression method is also a commonly used mathematical method [12, 13], but it has the shortcomings of low prediction accuracy and narrow application range. The main reason for these deficiencies is that these methods cannot capture the possible and complex nonlinear relationships between multiple factors.

The artificial neural network (ANN) is a common artificial intelligence prediction model. In recent years, it has gradually replaced the linear modeling method in the fields of financial time series prediction [14], machine failure prediction [15], and rainfall prediction [16]. An ANN model can determine the complex nonlinear mapping relationship between different variables through data training and then complete the prediction work. When an ANN model is applied to the subway ticket price prediction, a prediction model can be established using the factors influencing ticket price as the input and the fare as the output. The back-propagation (BP) feed-forward neural network can approximate any nonlinear function, so it is the most commonly used ANN algorithm [17]. However, in the process of using the BP neural network, there are often some problems, such as slow convergence speed, ease of falling into local minima, and poor robustness [18, 19].

At present, with the aim of addressing the above shortcomings of the BP algorithm, the genetic algorithm (GA), the particle swarm optimization (PSO), and other metaheuristic algorithms are often used to optimize the weights and thresholds of the BP neural network. Zou et al. [20] used the BP algorithm, optimized by the GA, to effectively identify the shear parameters of lunar rock mass. However, such study did not compare the calculation results of the GA with other optimization algorithms and did not conduct further research and analysis on the shortcomings of the GA, such as complex programming, complex parameter setting, and slow convergence speed [21]. Nasimi et al. [22] predicted the bottomhole pressure of drilling facilities by using the BP algorithm optimized by the PSO algorithm. Another study did not analyze the premature convergence and convergence to the local optimal solution of the PSO algorithm [23]. In 2020, Xu and Shen [24] proposed the sparrow search algorithm (SSA) referring to the biological phenomenon of the sparrow population foraging. The SSA can achieve higher global exploration ability and local development ability with the help of a flexible foraging and antipredation mechanism in the sparrow population.

As the SSA is quite new, there are few reports on its application in engineering problems and theoretical analysis. Xue and Shen [24] used the SSA, grey wolf optimizer (GWO), gravitational search algorithm (GSA), and PSO algorithms to calculate and analyze 19 typical optimization functions and two engineering problems. The calculation results showed that the SSA had the advantages of good stability, strong global search ability, and few parameters compared with other optimization algorithms. Lv et al. [25] solved the image segmentation problem by using the SSA method. Their case study showed that the SSA method had better definition than the classical image segmentation methods. Tang et al. [26] used the improved SSA algorithm to study the path planning of an unmanned aerial vehicle (UAV). Their study showed that the improved SSA algorithm was superior to the PSO algorithm, the beetle antennae search (BA), the whale optimization algorithm (WOA), and the GWO. According to the no-free-lunch (NFL) theory [27], the expected performance of each algorithm is the same for solving all optimization problems. In other words, the computing performance of the same optimization algorithm in different optimization problems may be quite different. Therefore, this study will use the SSA to optimize the BP model to test the optimization performance of the SSA in the BP model. To the best of our knowledge, there has been no study published on the optimization of the BP model using the SSA.

Besides the optimization of model parameters, the selection of the input characteristic variables is also a key factor to determine the prediction accuracy of the BP neural network model [28, 29]. In order to reduce the number of input variables of the BP neural network, Mao et al. [30] used principal component analysis (PCA) to screen 10 key factors affecting magnesite grade. The PCA is used to integrate the original influencing factors into a small number of irrelevant variables by linear combination. Xu et al. [31] used a regression model to select the variables with high correlation as the input variables to predict the snow surface reflectance spectra at different depths during snow melting. Xu et al. [32] obtained the key input variables for the BP prediction model of chlorophyll in water by the multiple linear regression method. Their research results were based on the correlation between variables and screening of the key input variables of the BP neural network prediction model, and there were the following drawbacks. (1) The variable screening results of these methods might not be ideal. When choosing input variables, the researchers often chose independent variables to avoid the correlation of variables, which made the screening effect of multivariate regression analysis and PCA with the correlation of variables as the core likely not good. (2) The variable screening results of these methods were not easily interpretable. They studied the data relationship of variables, which could well explain the linear or nonlinear relationship between variables but could not clearly evaluate the influence of the linear or nonlinear relationship between variables on the prediction results.

In view of the above shortcomings, the mean impact value (MIV) has been increasingly widely used in input variable screening in recent years. The MIV is used to screen the key input variables by evaluating the extent of the influence of each input variable relative to the output variable, which has a great influence on the output variable. Li et al. [33] used the MIV to effectively identify the key factors affecting the soil corrosion of carbon steel in China. Their case study showed that the key factors identified based on MIV were consistent with the actual situation of soil corrosion of carbon steel in China, and the prediction of soil corrosion of carbon steel based on MIV-BP had a good accuracy. However, this study did not compare the calculation results of the BP algorithm with those of other intelligent algorithms. Considering the numerous evaluation indexes of pollutants in bus stations, Xu et al. [34] screened the indexes by the MIV method to reduce the number of input variables for the subsequent BP neural network. Dai et al. [35] developed a MIV-GA-BP model to calculate the optimal values of coal pillars. In their model, the MIV was used to identify the key factors affecting the optimal solution of the coal pillar. Their case study showed that the prediction error of this model was less than 5%, and the calculation accuracy was higher than that of other common artificial intelligence algorithms.

By summarizing the existing research, in this paper we put forward the following key issues that need to be studied. (1) To date, most of the research results on PPP subway systems have been in the field of public management, and there has been almost no research on the prediction of the price for the PPP subway service, which is a typical operation and management problem. Rapid and accurate price prediction is crucial for the smooth operation of the PPP subway system. (2) In the study to determine the key input variables of the BP model, researchers often used multiple regression analysis or PCA methods to obtain the key input variables by analyzing the correlation between input variables. These selection methods are subjective, and the calculation results are not easily interpretable. Choosing quantitative analysis methods, such as the MIV method, might be a reasonable approach to effectively deal with the deficiency that there are many factors affecting the prediction of the fare for the PPP subway system service. (3) At present, the commonly used prediction methods based on contract price adjustment, regression analysis and BP, GA-BP, and PSO-BP models have many shortcomings, such as low prediction accuracy and being time-consuming. Using the SSA method to optimize the BP model provides a new idea for accurately and rapidly predicting the ticket price for the PPP subway system service.

Based on the above literature, this paper used the MIV method, the SSA, and the BP model to develop an intelligent prediction method of the ticket price for the PPP subway system, which had the following literature contributions. (1) Previous related studies rarely predicted the ticket price for the PPP subway system. In this paper, the conducted in-depth theoretical and case studies provided new insights into the operation and management of the PPP subway system. (2) Starting from the relationship between the subway ticket price and the supply and demand of the subway service, this study analyzed the related factors affecting its price adjustment and produced the data acquisition and processing methods of each input variable. The MIV method was used to determine the key factors affecting the ticket prices for Beijing Subway Line 4, Wuhan Metro Line 2, and Chengdu Metro Line 1. The investment return rate, the local GDP, the number of similar vehicles, the financial subsidies, and the loan interest rates were key factors for these three systems. This processing method also reduced the number of input variables for subsequent BP models. (3) Considering the shortcomings of BP neural network model, such as its slow convergence speed and ease of falling into local optimum, this study, for the first time, used the SSA to optimize initial weights and thresholds and effectively solved these problems. (4) The case study showed that, compared with the traditional prediction method (the price adjustment method based on the PPP contract, the multiple regression analysis, the traditional BP, the GA-BP, and the PSO-BP), the calculation results of the model proposed in this paper had better prediction accuracy and stability.

The remainder of this paper is arranged as follows. In Section 2, the input variable system and the prediction model of the ticket price for the PPP subway system service are studied in detail. In Section 3, the prediction model is applied to Beijing Subway Line 4, Wuhan Metro Line 2, and Chengdu Metro Line 1. In addition, Section 3 describes the analysis of the nonlinear relationship between the variables to highlight the need to use the BP model. In Section 4, the calculation results of the different prediction models are compared, and the analysis of the key parameters of the MIV method is described. Section 5 summarizes the study and gives the research directions that warrant further study.

2. Materials and Methods

2.1. Input Variable System for Price Prediction of the PPP Subway System

2.1.1. Analysis of Factors Influencing the Ticket Price for the PPP Subway System. According to the definition and classification of public goods in economics, subway service belongs to quasi-public goods [36]. Under the PPP mode, the public (customer) can be regarded as the demand side of the subway service, while the supply side is the government departments and private investors who partnered with each other through concession contracts. Discussing the factors that affect the ticket price for the PPP subway service from the perspective of supply and demand can comprehensively consider the interests of the public, government departments, and private investors, which is more conducive to the smooth operation of the PPP subway system [37].

The greater the demand by the public for the subway service, the greater the transportation volume of the subway system, and the lower the ticket price. From the perspective of the demand of the subway service, there are three main factors that may affect the ticket price for the PPP subway service. (1) The number of potential subway passengers is determined by the number of urban residents and the local gross domestic product (GDP), and its size change has a great impact on subway service demand. The greater the number of urban residents, the greater the local GDP and the greater the subway demand. (2) The existence of similar means of transportation will divert to a certain extent the number of subway passengers, who will choose according to the change of the transportation price. Generally speaking, the lower the price of subway tickets, the fewer the similar means of transportation and the greater the demand for the subway service. (3) The satisfaction of the public with the subway service quality will also affect the demand for the subway service, such as subway congestion, on-time departure, on-time arrival, and safety.

From the perspective of the supply side, the ticket price for the PPP subway service is the result of the cooperation and game between government agencies and private investors [38]. This study does not delve into the complex game process between the two sides but rather analyzes the factors that may affect the ticket price for the PPP subway service from the following three perspectives. (1) Due to the public welfare aspect of the subway service, the government has strict supervision over subway service prices, and it is impossible for private investors to recover their investment through ticket revenue, thus subsidies have a great impact on the revenue of private investors [39]. In general, the greater the government subsidy, the lower the fare of the PPP subway system. (2) The construction and operation costs of the subway project have a direct impact on the revenue of the system. As the cooperation period of the PPP subway system is often as long as 30 years, the loan interest rate of construction loans [40] and inflation during the operation period [41] have a great impact on the cost of PPP subway systems. When the project cost increases, the private capital will increase the price of the ticket to ensure the revenue of system. (3) The expectation of investment revenue from the PPP subway system by the private investors also has great influence on ticket price. The higher the expected return on the investment, the higher the price of the ticket. Moreover, from the macro environment, due to the long operation period of the PPP subway system, the introduction of relevant national policies and laws will cause changes in the demand or supply of the PPP subway service during the operation period [41]. Therefore, it will cause fluctuations in subway ticket prices.

2.1.2. Selection and Quantification Method of Input Variables for the Prediction of Prices for the PPP Subway Service. According to the research results of Section 2.1.2, based on the scientificity, representativeness, and independence provisions and taking into account the availability and operability data of the PPP subway system, the following eight variables are selected as the input variables for the prediction of the ticket price for the PPP subway service, as shown in Table 1.

The value of $X8$ was obtained through a questionnaire survey. In the questionnaire for $X8$, $[0, 25)$ indicated dissatisfaction, $[25, 50)$ indicated dissatisfaction, $[50, 75)$ indicated basic satisfaction, and $[75, 100)$ indicated satisfaction. The $X2$, $X4$, and the output variable can be in the same currency unit, such as RMB, USD, or EUR.

Each input variable in Table 1 is normalized based on (1) to ensure the calculation accuracy of the subsequent prediction model, as reported in [31].

$$x_i^* = \frac{x_i - x_{\min}}{x_{\max} - x_{\min}}, \tag{1}$$

where x_i^* is the normalized value, x_i is the i-th value of input variable x, $x_{\max}$ is the maximum value of input variable x, and $x_{\min}$ is the minimum value of input variable x.

Table 1: Input variables for the prediction of the ticket for the PPP subway systems.

Input variable	No.	Unit	Data acquisition method
Number of local people	$X1$	Million	Access to government notices
Total local GDP	$X2$	Billion	Access to government notices
Number of similar vehicles	$X3$	—	On-site investigation or access to government announcements
Financial subsidy	$X4$	Million	Access to government notices
Loan interest rate	$X5$	%	Check on the project management data
Inflation rate	$X6$	%	Access to statistical data
Rate of return on investment	$X7$	%	Check on the project management data
Public satisfaction	$X8$	RMB/km	Questionnaire survey

2.2. Intelligent Prediction Method of Ticket Price for the PPP Subway Service

2.2.1. Introduction to the BP Model. As a typical feed-forward neural network, the BP neural network is mainly used in nonlinear learning, pattern recognition and classification, system control, and other fields [15]. The BP neural network takes the input data as learning samples, adjusts the weights and thresholds of the whole network by the back-propagation algorithm, constructs a mapping relationship between input and output that is closest to the sample, and uses this mapping relationship to predict the output value. Based on the black box theory, this method simulates the structure and function of a neural network in the human brain and can solve any nonlinear mapping process without constructing a specific mathematical formula, which has the characteristics of good adaptability, high fault tolerance, and strong nonlinear processing ability [15, 16].

MLP is a multilayer fully connected feed-forward network, which is only an algorithm structure. After the samples are input, the samples are fed forward layer by layer in the MLP network (from the input layer to the hidden layer and to the output layer, the results are calculated layer by layer, that is, the so-called feed-forward), and the final output value is obtained. However, the connection coefficients and offsets of neurons in each layer of MLP need training and optimization, and the BP is often used to get the coefficients and offsets in the model. Strictly from the field of algorithm research, the reviewer's statement is more accurate. The neural network is MLP, and the BP neural network (BP-MLP) is an MLP network optimized by BP algorithm.

A complete BP neural network model usually includes three basic network structures, namely, the input layer, hidden layer, and output layer [15]. Taking the process of ticket price prediction for the PPP subway service as an example, the basic structure of the BP neural network model is shown in Figure 1.

Combined with the diagram shown in Figure 1, the construction process of the BP neural network in this paper is as follows.

The input vector $X = (x_1, x_2, \ldots, x_n)$ and the output variable $Y = (y)$ are brought into the BP neural network, and the output values of each unit in the hidden layer [15] are

$$Z_j = F\left(\sum_{i=1}^{n}\left(w_{ij}x_i - b_j\right)\right), \tag{2}$$

where Z_j is the input value of the hidden layer; w_{ij} and b_j are, respectively, the connection weights and thresholds of input layer and hidden layer; i is the dimension of the input layer, $i = 1, 2, \ldots, n$; and j is the dimension of hidden layer, $j = 1, 2, \ldots, n$. F is the activation function of the hidden layer.

The output value of each unit in the output layer is calculated by using the connection weight w_{ij} and threshold b_j of the hidden layer and the output layer as reported in [15]:

$$O_t = G\left(\sum_{j=1}^{m}\left(w_{tj}F\left(\sum_{i=1}^{n}\left(w_{ij}x_i - b_j\right)\right) - b_t\right)\right), \tag{3}$$

where O_t is the output value of the output layer, t is the dimension of the output layer, $j = 1, 2, \ldots, l$, and G are the activation functions of the output layer.

Therefore, the sum of the error squares of the output vector O and the actual value Y of the ticket price is as previously reported [15, 16]:

$$E = \frac{1}{2}\sum_{t=1}^{l}\left(y_t - O_t\right)^2. \tag{4}$$

Gradually extending backward to the hidden layer and the input layer, we can further calculate and obtain (5) as reported in [14, 15]:

$$E = \frac{1}{2}\sum_{t=1}^{l}\left(y_t - G'\left(\sum_{j=1}^{m}\left(w_{jt}F'\left(\sum_{i=1}^{n}\left(w_{ij}x_i - b_j\right)\right) - b_t\right)\right)\right)^2, \tag{5}$$

where F' and G' are the inverse functions of activation functions F and G, respectively.

According to the principle of minimum error, the gradient descent method is adopted, and through iterative solution, connection weights, and thresholds of the input layer and hidden layer, the hidden layer and output layer are corrected item by item, so that the final output result of the neural network approaches the expected output value, thus reaching the preset value of the error square sum E.

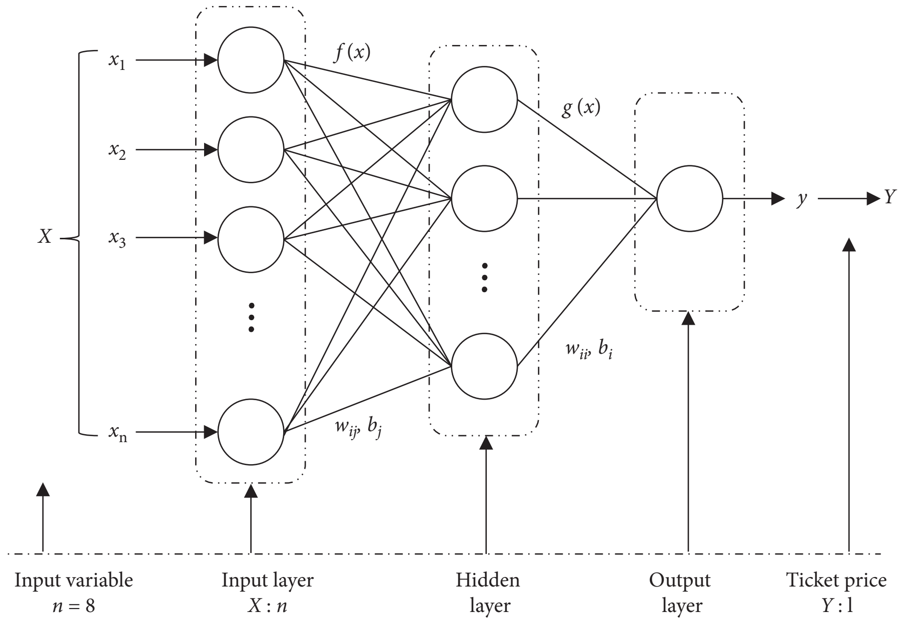

FIGURE 1: Structure diagram of the neural network.

2.2.2. Introduction to SSA. The SSA was proposed in 2020. SSA is mainly inspired by the sparrows' foraging behavior and antipredation behavior. This is a novel algorithm that has the advantages of strong optimization ability and fast convergence speed. The SSA is used to optimize the initial weights of the BP neural network and develop the SSA-BP model, which not only makes full use of the mapping ability of the BP neural network, but also has the rapid global convergence and learning ability of the SSA.

Considering that the SSA is quite new, this paper introduces the main rules of the SSA in detail as reported in [24], so that the readers can better understand the research content of this paper:

Rule (1). The discoverer usually has a high energy reserve and is responsible for searching for areas rich in food in the whole environment, providing foraging areas and directions for all participants. In the development of the model, the level of energy reserve depends on the fitness value of sparrows.

Rule (2). Once sparrows find predators, individuals start to sing as alarm signals. When the alarm value is greater than the safe value, the discoverer will take the participants to other safe areas for foraging.

Rule (3). The identities of the discoverers and entrants are dynamically changing. As long as we can find a better food source, every sparrow can become a discoverer, but the proportion of discoverers and entrants in the total population remains unchanged.

Rule (4). The lower the energy of the participants, the worse their foraging position in the whole population. Some hungry entrants are more likely to fly to other places to find food for more energy.

Rule (5). In the process of foraging, participants can always search for the discoverer that provides the best food and then get food from the best food source or forage around the discoverer. At the same time, in order to increase their predation rate, some participants may constantly monitor the discoverers and compete for food resources.

Rule (6). When being aware of the danger, sparrows at the edge of the population will quickly move to a safe area to get a better position, while sparrows in the middle of the population will fly randomly to get close to other sparrows.

According to the above rules, when using virtual sparrows to search for food, the population composed of n sparrows can be expressed [24] as follows:

$$\mathbf{X} = \begin{bmatrix} x_{11} & x_{12} & \cdots & x_{1d} \\ x_{21} & x_{22} & \cdots & x_{2d} \\ \cdots & \cdots & \cdots & \cdots \\ x_{n1} & x_{n2} & \cdots & x_{nd} \end{bmatrix}, \tag{6}$$

where d denotes the dimension of the problem variable to be optimized and n is the number of sparrows.

The fitness values of all sparrows can be expressed [24] as follows:

$$\mathbf{F}_x = \begin{bmatrix} f\left(\left[x_{11} \;\; x_{12} \;\; \cdots \;\; x_{1d}\right]\right) \\ f\left(\left[x_{21} \;\; x_{22} \;\; \cdots \;\; x_{2d}\right]\right) \\ \cdots \\ f\left(\left[x_{n1} \;\; x_{n2} \;\; \cdots \;\; x_{nd}\right]\right) \end{bmatrix}, \tag{7}$$

where f denotes fitness.

In the SSA, the discoverer with better fitness value will get food first during the search process. In addition, the discoverer is responsible for finding food for the whole sparrow population and providing foraging directions for all participants. Therefore, the discoverer can obtain a larger foraging search range than the entrant. According to Rule (1) and Rule (2), $R_2 < \mathrm{ST}$ means that there are no predators around the foraging environment at that time and the discoverer can perform extensive search operations. $R_2 \geq \mathrm{ST}$ means that some sparrows in the population have found predators and sent an alarm to other sparrows in the population. At this time, all sparrows need to rapidly fly to other safe places for foraging.

During each iteration, the location update of the discoverer is described [25] as follows:

$$\mathbf{X}_{i,j}^{t+1} = \begin{cases} \exp\left(-\dfrac{1}{\alpha * \mathrm{item}_{\max}}\right) * \mathbf{X}_{i,j}^{t}, & \text{if } R_2 < \mathrm{ST}, \\ \mathbf{X}_{i,j}^{t} + Q * \mathbf{L}, & \text{if } R_2 \geq \mathrm{ST}, \end{cases} \tag{8}$$

where t represents the current iteration number, $j = 1, 2, 3, \ldots, d$, and $\mathrm{item}_{\max}$ denotes the maximum iteration number. $\mathbf{X}_{i,j}^{t}$ indicates the position information of the i-th sparrow in the j-th dimension in the t-th iteration, and α represents a random number less than or equal to 1 but greater than 0. $R_2\,(R_2 \in [0,1])$ and $\mathrm{ST}\,(\mathrm{ST} \in [0.5,1])$ represent the warning value and the safety value, respectively. Q is a random number that obeys normal distribution. $\mathbf{L}$ denotes a $1 \times d$ matrix, in which every element in the matrix is 1.

For the participants, they need to execute Rule (3) and Rule (4). As described above, during the foraging process, some participants will keep an eye on the discoverer. Once they perceive that the discoverer has found better food, they will immediately leave their present position to compete for food. If they win, they can get the food of the discoverer immediately; otherwise, they need to continue to execute Rule (4). When $i > 0.5n$, this indicates that the i-th participant with low fitness value does not have food and is in a very hungry state. At this time, it is necessary to fly to other places for food to get more energy. The location update of the enrolee is described [24, 25] as follows:

$$\mathbf{X}_{i,j}^{t+1} = \begin{cases} Q * \exp\left(\dfrac{\mathbf{X}_{\mathrm{worst}} - \mathbf{X}_{i,j}^{t}}{i^2}\right), & \text{if } i > 0.5n, \\ \mathbf{X}_{P}^{t+1} + \left|\mathbf{X}_{i,j} - \mathbf{X}_{P}^{t+1}\right| \cdot \mathbf{A}^{+} \cdot \mathbf{L}, & \text{otherwise}, \end{cases} \tag{9}$$

where $\mathbf{X}_P$ is the best position occupied by the discoverer at the moment and $\mathbf{X}_{\mathrm{worst}}$ represents the worst position in the world at the moment. $\mathbf{A}$ represents a $1 \times d$ matrix, in which each element is randomly assigned 1 or −1, and $\mathbf{A}^{+} = \mathbf{A}^{\mathrm{T}}(\mathbf{A}\mathbf{A}^{\mathrm{T}})^{-1}$.

In the simulation experiment, we assume that the sparrows aware of danger account for 10% to 20% of the total population. The initial positions of these sparrows are randomly generated in the population. According to Rule (5), $f_i > f_g$ means that the sparrows are at the edge of the population at that time and are extremely vulnerable to predators. $\mathbf{X}_{\mathrm{best}}$ indicates that the sparrow at that position is at the best position in the population and is very safe. When $f_i = f_g$, it shows that sparrows in the middle of the population are aware of the danger and need to approach other sparrows to minimize the risk of predation.

The specific mathematical expression can be written [24, 26] as follows:

$$\mathbf{X}_{i,j}^{t+1} = \begin{cases} \mathbf{X}_{\mathrm{best}}^{t} + \beta * \left|\mathbf{X}_{i,j}^{t} - \mathbf{X}_{\mathrm{best}}^{t}\right|, & \text{if } f_i > f_g, \\ \mathbf{X}_{i,j}^{t} + K * \left(\dfrac{\left|\mathbf{X}_{i,j}^{t} - \mathbf{X}_{\mathrm{worst}}^{t}\right|}{(f_i - f_w) + \varepsilon}\right), & \text{if } f_i = f_g, \end{cases} \tag{10}$$

where $\mathbf{X}_{\mathrm{best}}^{t}$ is the current global optimal position. β, as a step control parameter, is a random number that obeys the standard normal distribution. $K \in [0,1]$ is a random number, which indicates the moving direction of sparrows and is also a step control parameter. f_i is the fitness value of individual sparrows. f_g and f_w are the best and worst fitness values, in the world, respectively. ε is used to avoid having zero in the denominator.

2.2.3. Introduction to the MIV Method. The MIV method proposed by Dombi et al. [42] is considered as one of the best indexes to evaluate the correlation of variables in neural networks. The basic idea of applying the MIV method to the model developed in this study is to take the variables with a significant impact on the price of the ticket for the PPP subway system as the input parameters of the prediction model and to eliminate the variables that have less impact.

The specific implementation method of the MIV method is as follows:

Step 1. The training samples to train the SSA-BP neural network are selected, and the prediction model Ptrain is obtained.

Step 2. Each characteristic variable in sample $\mathbf{T}$ is increased or decreased by 10%, and the new samples $\mathbf{T}_1$ and $\mathbf{T}_2$ are obtained. Samples $\mathbf{T}_1$ and $\mathbf{T}_2$ are then regressed with the aid of the model Ptrain, and the regression results $\mathbf{A}_1$ and $\mathbf{A}_2$ are obtained.

Step 3. $\mathbf{E} = \mathbf{A}_1 - \mathbf{A}_2$ is taken as the change value that influences the output result after the characteristic variable changes, and the MIV is obtained by averaging $\mathbf{E}$ according to the number of samples. According to the MIV value, the extent of the influence of each characteristic variable on ticket price is obtained.

Step 4. The relative contribution rate of each variable α_i is calculated [24] as follows:

$$\alpha_i = \frac{\left|\mathrm{MIV}_i\right|}{\sum_{i=1}^{n}\left|\mathrm{MIV}_i\right|}, \tag{11}$$

where MIV_i is the MIV value of the i-th index.

Step 5. Input variables with relative contribution rate greater than 10% are selected as key input variables.

2.2.4. Prediction Model Based on the MIV-SSA-BP. The basic flow chart of the SSA-BP model is shown in Figure 2, and the input variable screening method based on the MIV is shown in Figure 3. The prediction model proposed in this paper is mainly divided into three parts. (1) All input variables are brought into the fare prediction model based on the SSA-BP. (2) The MIV method is used to obtain the key variables. (3) The key variables are brought into the SSA-BP to predict the ticket price again.

It should be emphasized that the mathematical model constructed in this paper can be applied to the study of complex and nonlinear data prediction. If the input and output variable system constructed in this paper is adopted, the model proposed in this paper can quickly and accurately predict the price of subway PPP project.

The calculation steps of the intelligent prediction method proposed in this paper are as follows:

Step 1. The input data is normalized by (1).

Step 2. The learning parameters of the SSA and BP algorithm are determined according to the size and characteristics of the learning samples. Equation (6) is used to initialize the predator and joiner. Then, (2)–(5) are used to initialize the BP neural network. The detailed construction process of the BP neural network is shown in Section 2.2.1.

Step 3. The fitness value of each virtual sparrow is calculated by (7) and then sorted. The positions of the discoverer, joiner, and watcher are updated with (8)–(10), respectively.

Step 4. The fitness value is calculated and the sparrow position is updated.

Step 5. Whether the stop condition is met is determined; if yes, then exit and output the result. Otherwise, Steps 3–4 are repeated.

Step 6. The MIV method described in Section 2.2.3 is used to calculate and obtain the key input variables.

Step 7. Finally, Steps 2–5 are reexecuted, and the obtained key input variables are brought into the SSA-BP model to obtain the final output result.

3. Case Study

3.1. Data Sources. In this paper, Beijing Subway Line 4, Wuhan Metro Line 2, and Chengdu Metro Line 1, three typical PPP subway systems, were selected as case studies. Beijing Metro Line 4 was put into trial operation on September 28, 2009. As of October 1, 2020, the private capital investors and government agency have adjusted the price 10 times. Wuhan Metro Line 2 was put into operation on December 28, 2012. As of October 1, 2020, Wuhan Metro Line 2 has a total length of 60.8 kilometres, with an average daily passenger flow of more than 150,000 passengers. During the operation period, the private capital investors and government agency have adjusted the price six times. Chengdu Metro Line 1 was put into operation on September 27, 2010. As of October 1, 2020, Chengdu Metro Line 1 has a total length of 41 kilometres, with a total of 35 stations, with the highest single-day passenger traffic of 1,091,900 passengers on February 19, 2019. During the operation of Chengdu Metro Line 1, the private capital investors and the government agency adjusted the price nine times.

Using the index acquisition method of each input variable shown in Table 1, the 25 price adjustment data sets of the three PPP subway systems are obtained as shown in Table 2.

In Table 2, the monetary unit of $X1$, $X2$, and $X4$ is RMB. The $X5$ loan interest rate is the five-year national debt interest rate issued by the Chinese government. The $X6$ is expressed by the consumer price index (CPI) published by the Chinese government. The $X8$ data is directly derived from the questionnaire survey results provided by the PPP Project Company of Metro.

3.2. Correlation Analysis of Various Variables. In order to study the linear correlation between the input variables and the output variable (the ticket price), the Pearson correlation analysis method is used to quantitatively describe the degree of linear correlation between the parameters [43]. The detailed calculation principle and method used have been previously reported [43]. The closer the Pearson correlation coefficient (r) is to 1, the stronger the linear correlation between the two indicators. When the r is equal to 0, there is no linear correlation between the two indicators. When the r is positive, the indicators are positively correlated, and when r is negative, they are negatively correlated; r is defined as

$$r = \frac{\sum_{i=1}^{n}\left(x_i - \overline{x}\right)\left(y_i - \overline{y}\right)}{\sqrt{\sum_{i=1}^{n}\left(x_i - \overline{x}\right)^2\left(y_i - \overline{y}\right)^2}}, \tag{12}$$

where x_i is the value of an input variable, $\overline{x}$ is the average value of an input variable, y_i is the value of another input variable, and $\overline{y}$ is the average value of another input variable.

Substituting the data in Table 2 into (12), the obtained calculation results are shown in Table 3. In Table 3, the absolute value of the values in bold is greater than 0.8, which indicates that there is a significant correlation between these two indicators.

According to the calculation results listed in Table 3, among the 8 input variables of the ticket price prediction of the PPP subway system, the linear relationship between the indexes is mostly weak. However, $X2$ and $X4$ have a correlation coefficient of 0.812, $X4$ and $X7$ have a correlation coefficient of 0.857, and $X5$ and $X6$ have a correlation coefficient of 0.894, which indicates that these variables have a certain positive linear correlation between them. The correlation coefficient between $X5$ and $X7$ is −0.840, and the correlation coefficient between $X6$ and $X7$ is −0.913, which indicates that there is a certain negative linear correlation between these variables. The absolute values of other correlation coefficients are all lower than 0.8, indicating that their linear correlation is quite weak. Therefore, when using the input variables constructed in Section 2.1 of this paper to predict the PPP subway tickets, the nonlinear modeling method should be favored [28].

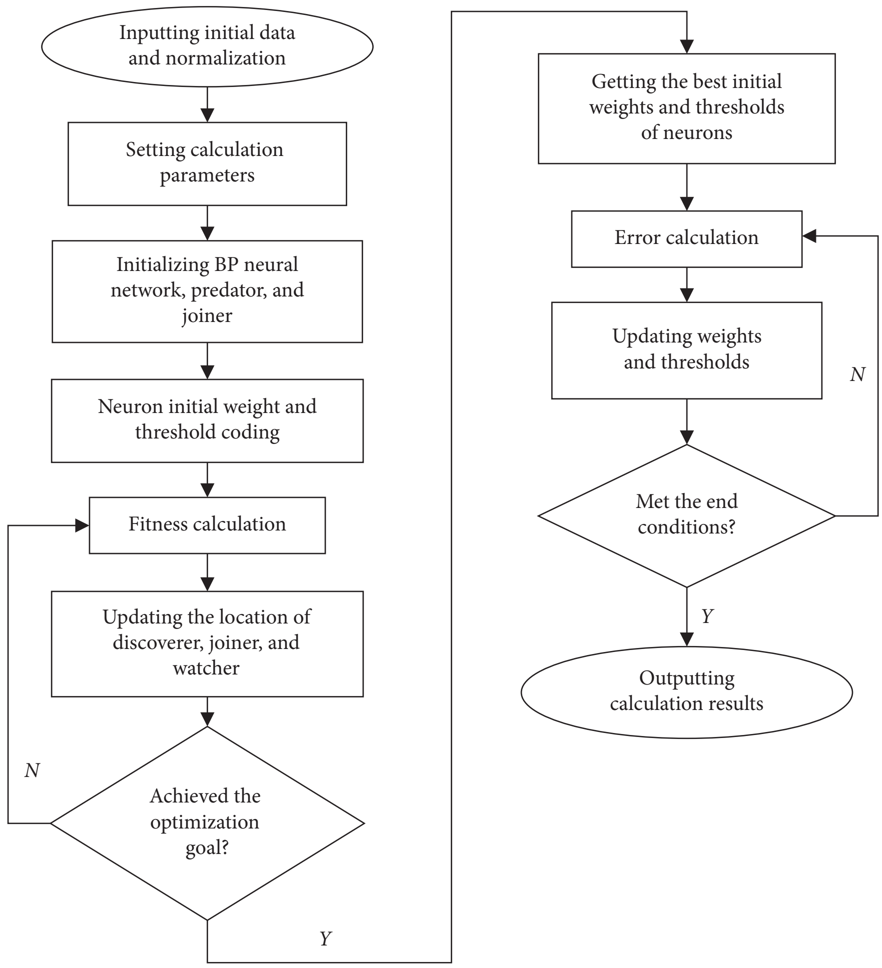

Figure 2: Flow chart of the SSA-BP model.

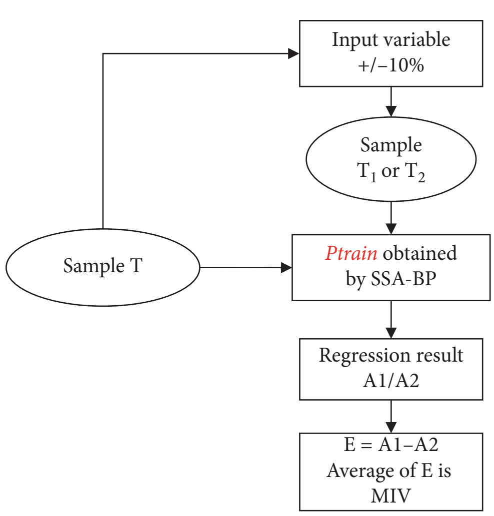

Figure 3: Flow chart of the MIV method.

3.3. Ticket Price Forecast Based on SSA-BP. In the modeling process of the SSA-BP, data sets can be divided into training sets and test sets. Among them, the training data set is used to train the model, while the test data set is used to evaluate the model. The ratio between the common training data set and test set is 90 : 10%, 80 : 20%, or 70 : 30% [44]. Considering that there are 25 data sets in this paper, the first 20 samples are set as the training data set, and the last 5 samples are set as the test data set. In other words, the ratio between training data set and test data set in this paper is 75 : 25%.

In this study, three indexes, namely, the mean absolute percentage error (MAPE), the root mean square error (RMSE), and the coefficient of determination (R^2), are used to evaluate the calculation accuracy of the prediction model.

The value of the MAPE is 0%, indicating that the prediction result is perfect [45]. If the MAPE is greater than 100%, it is generally considered that the prediction result is unavailable. MAPE is defined as follows:

$$\text{MAPE} = \frac{1}{n}\sum_{i=1}^{n}\left|y_i - \dot{y}_i\right|, \tag{13}$$

where n is the number of sample points, y_i is the predicted value of the ticket price of the PPP subway system, and $\dot{y}_i$ is the actual value.

The RMSE [46] can directly reveal the average error between the predicted value and the true value, and when the predicted value is completely consistent with the true value,

Table 2: Engineering data.

No. (unit)	$X1$ (million)	$X2$ (billion)	$X3$	$X4$ (million)	$X5$ (%)	$X6$ (%)	$X7$ (%)	$X8$	Y (RMB/km)
1	19.612	1411.360	4	138.800	4.39	2.9	8	77	0.37
2	20.186	1625.190	5	156.000	4.40	1.3	7	60	0.37
3	20.693	1780.102	5	173.200	4.42	1.4	6.8	82	0.38
4	20.693	1780.102	6	178.800	4.42	1.7	7	83	0.42
…	…	…	…	…	…	…	…		…
24	16.330	1534.277	7	217.000	4.40	4.5	5.5	87	0.48
25	16.581	1701.265	9	223.500	4.42	4.9	6.5	80	0.50

Table 3: Pearson correlation coefficient between indexes.

Factor	$X1$	$X2$	$X3$	$X4$	$X5$	$X6$	$X7$	$X8$
$X1$	1.000	0.514	0.231	0.423	0.123	−0.362	0.378	0.271
$X2$	—	1.000	0.482	**0.812**	−0.381	−0.575	0.432	0.154
$X3$	—	—	1.000	**−0.834**	0.041	0.234	0.340	0.299
$X4$	—	—	—	1.000	0.104	0.246	**0.857**	0.430
$X5$	—	—	—	—	1.000	**0.894**	**−0.840**	0.255
$X6$	—	—	—	—	—	1.000	**−0.913**	0.129
$X7$	—	—	—	—	—	—	1.000	−0.311
$X8$	—	—	—	—	—	—	—	1.000

Bold values mean that the absolute value is greater than 0.8.

it is equal to 0, that is, the perfect model. The larger the error, the larger the value. The RMSE is defined as shown in (14), which can be used to calculate it, as follows:

$$\mathrm{RMSE} = \sqrt{\frac{1}{n}\sum_{i=1}^{n}\left(y_i - \dot{y}_i\right)^2}. \tag{14}$$

The closer the value of R^2 [47] is to 1, the better the prediction result is. The result obtained here is 0, indicating that the model fitting effect is very poor.

$$R^2 = 1 - \frac{\sum_{i=1}^{n}\left(y_i - \dot{y}_i\right)^2}{\sum_{i=1}^{n}\left(y_i - \overline{y}_i\right)^2}, \tag{15}$$

where $\overline{y}_i$ is the average value of the predicted values.

In the SSA proposed in this paper, the population size is set to $n = 50$, the maximum number of iterations is 200, the safety threshold ST = 0.8, discoverers account for 20% of the population size, and the number of sparrows aware of danger SD = 5. The experimental environment is as follows: the simulation experiment was performed in the Matlab 2016a on a 3.40 GHz Intel i7 processor and a computer with 16 GB memory.

In this study, the BP neural network is trained by the Levenberg–Marquardt algorithm. The maximum training times are 200, the coefficient of motion vector is 0.3, and the minimum mean square error is 10^{-5}.

The activation functions of the hidden layer and output layer, respectively, adopt the logsin function $F(x)$ and purelin linear function $G(x)$, shown as follows:

$$\begin{aligned} F(x) &= \frac{1}{1+e^{-x}}, \\ G(x) &= x. \end{aligned} \tag{16}$$

The number of nodes in different hidden layers may have an impact on the BP prediction results. Therefore, this study calculates the calculation error of the prediction model under different hidden layer nodes. According to past research studies [20, 22], the number m of hidden layer nodes is selected according to the following empirical equation:

$$m = \sqrt{n+l} + \delta, \tag{17}$$

where δ is a constant in the range of 1–10, n is the dimension of hidden layer, and l is the dimension of the output layer.

Substituting $n = 8$ and $l = 1$ into (17), we can obtain $m = 4, 5, \ldots, 13$. In order to find the optimal value of the hidden layer node m, the SSA-BP neural network is trained with $m = 4, 5, \ldots, 13$, and the training results are compared. The calculation results are shown in Table 4. In Table 4, the values in bold indicate the calculation results with the highest calculation accuracy.

The data in Table 4 reveal that when the number of hidden layer neuron nodes is $m = 6$, the MAPE and RMSE are the smallest and R^2 is the largest, and the BP neural network is the most accurate algorithm to predict the ticket price for the PPP subway service. Therefore, the number of hidden layer nodes in the SSA-BP model is ultimately determined to be 6.

The data in Table 4 show that when all variables affecting the prediction of the ticket price for the PPP subway service are taken as the input parameters of the SSA-BP neural network model, the calculation accuracy reaches 95.59%, which still does not meet the practical application requirements. Considering that the input variables may have influence on the prediction accuracy of the BP neural network model, the key variables are screened out by this method, and the calculation results are shown in Table 5.

The data in Table 5 reveal that 8 input variables have different effects on the prediction of the ticket price for the

Table 4: Effect of the number of nodes in different hidden layers on the prediction.

Number of hidden layer nodes	MAPE (%)	RMSE	R^2 (%)
4	4.213	0.029	93.23
5	3.487	0.022	94.31
6	**2.912**	**0.018**	**95.59**
7	4.781	0.027	92.65
8	6.573	0.029	90.46
9	7.378	0.023	88.10
10	9.958	0.030	86.02
11	8.260	0.0300	88.35
12	6.317	0.026	91.13
13	4.098	0.023	93.49

The numerical value in bold represents the calculation result with the highest calculation accuracy.

Table 5: Calculation results of the input variables based on MIV.

Variables	MIV	Order	Relative contribution rate (%)	Cumulative contribution rate (%)
*X*7	0.071	1	28.63	28.63
*X*2	−0.053	2	21.37	50.00
*X*3	0.046	3	18.55	68.55
*X*4	0.032	4	12.90	81.45
*X*5	−0.027	5	10.89	92.34
*X*6	0.014	6	5.65	97.98
*X*1	−0.003	7	1.21	99.19
*X*8	0.002	8	0.81	100.00

PPP subway service. The MIV values of *X*2, *X*5, and *X*1 are all negative, which indicates that these three input variables are negatively correlated with the ticket price. Other indicators are positively correlated with the ticket price. The relative contribution rates of *X*7, *X*2, *X*3, *X*4, and *X*5 are all higher than 10%, while the relative contribution rates of the remaining input variables are lower than 10%. Therefore, in this case study, *X*7, *X*2, *X*3, *X*4, and *X*5 are selected as the key input variables for the prediction of the ticket price for the PPP subway service.

The *X*7, *X*2, *X*3, *X*4, and *X*5 are brought back into the prediction model based on the SSA-BP model, and some parameter settings are almost unchanged. However, since the input variables have changed, the number of hidden layer nodes needs to be redetermined. According to empirical equation (17), when the number of hidden layer neuron nodes is $m = 5$, the MAPE (2.381%) and RMSE (1.4780) are the smallest and R^2 (97.31) is the largest, and the BP neural network is the most accurate to predict the ticket price for the PPP subway service. The chart of the error loss function is shown in Figure 4.

To further clarify the optimization calculation process of SSA, detailed optimization calculation process is shown in Table 6.

According to the calculation results shown in Figure 4 and Table 6, the fitness of the SSA rapidly decreases in the initial stage (about 20–55 generations). Then, with the increase of the number of iterations, the fitness eventually converges to 45.31411. This shows that the SSA effectively optimizes the BP model. Comparison with the convergence curves of the GA and PSO algorithm indicates that the SSA has faster convergence speed. The analysis of the calculation results of the different algorithms will be shown in detail in Section 4.1.

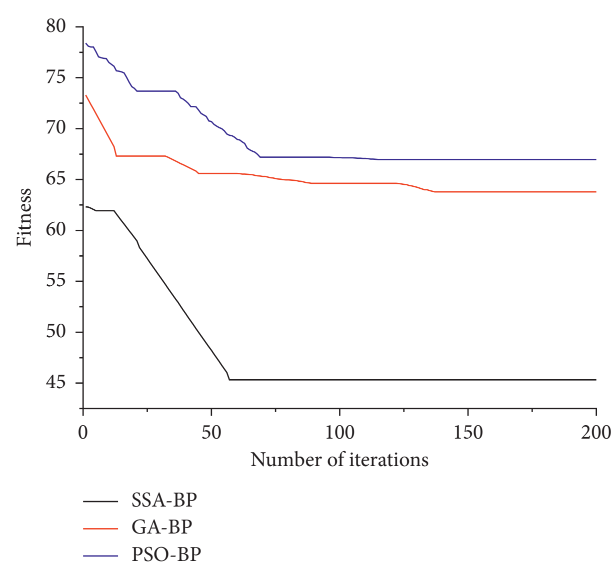

Figure 4: Chart of the fitness.

The Bland–Altman analysis of the predicted and measured ticket prices [48], shown in Figure 5, reveals that the predicted values of five groups of ticket prices are within (−1.96SD, +1.96SD). Thus, according to the Bland–Altman analysis method, 95% of the predicted points are within the consistent range. Therefore, considering the application of ticket price prediction, the prediction method developed in this study is feasible.

The 10-fold cross-validation method is often used to test the accuracy of algorithms. The basic idea is to divide the data set into ten parts, and take turns to take 9 parts as

Table 6: Detailed optimization calculation process.

Iteration (n)	Fitness (n–1)	Fitness (n)	Fitness (n)–fitness (n–1)	Result
56	46.39730	46.03623	0 < 0.00001	Continue
57	46.03623	45.31411	0.361063611 > 0.0001	Continue
58	45.31411	45.31411	0 < 0.0001	Continue
200	45.31411	45.31411	0 < 0.0001	Stop

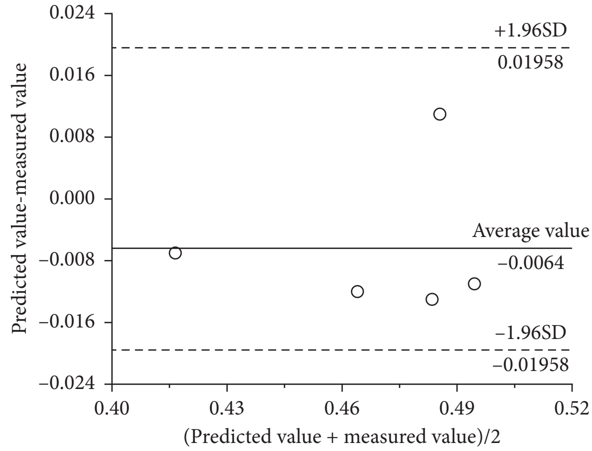

Figure 5: Bland–Altman analysis of the predicted values and actual values.

Table 7: Calculation results of the 10-fold cross-validation.

No.	1	2	3	4	5	6	7	8	9	10
MAPE (%)	2.38	2.45	2.94	2.57	2.01	2.50	1.95	2.48	3.14	2.63
RMSE	0.014	0.015	0.015	0.015	0.014	0.015	0.014	0.014	0.015	0.015
R^2 (%)	97.31	96.45	97.58	96.85	95.97	96.79	97.30	96.43	97.52	97.93

training data and 1 part as test data for experiments. In this paper, the 10-fold cross-validation method is used to test the accuracy of the proposed model, and the calculation results are shown in Table 7.

The calculation data in Table 7 indicate that the ten prediction results have good prediction accuracy and calculation stability. These findings show that the calculation results of the case analysis are accurate and no overfitting phenomenon occurs.

4. Discussion

Based on the MIV method, the SSA, and the BP algorithm, this study developed an intelligent prediction method of the ticket price for a PPP subway system. However, this study has the following three limitations: (1) The definition of the ticket price for the PPP subway system in the introduction of this paper is the ticket price when the government and private capital investors play a game, not the actual ticket price for the customers. Different definitions of the ticket price may influence the research results of this study. (2) More novel algorithms, such as chaotic local search-based differential evolution algorithm (CLSDEA) [49], can be used to optimize the BP model. (3) The calculation parameter setting of optimization algorithm has obvious influence on the calculation efficiency of optimization algorithm [50, 51], but this paper has not completed the relevant analysis.

4.1. Analysis of the Calculation Accuracy of Different Prediction Models. The research results in the third section of this paper show that the prediction model proposed in this paper has high accuracy and stability. However, these research results can only confirm the validity of the model proposed in this paper. In order to further analyze the advancement of the model proposed in this paper, in this section we compare various prediction methods, including price adjustment method based on PPP contract, multiple regression, BP, GA-BP, PSO-BP, and support vector machine (SVM).

According to the historical data of three subway station projects, the price adjustment results based on the PPP contract were obtained and are shown in Table 8. In engineering practice, every price adjustment based on contract took about 1-2 months.

When multiple regression analysis was adopted, the first 20 groups of data of 8 input variables were all brought in. According to the calculation of Excel 2016 software, the relationship between 8 input variables and output variable was

Table 8: Comparison of calculation results of different models with 8 input variables.

Error representations	MAPE (%)	RMSE	R^2 (%)
Price adjustment method based on PPP contract	49.375	0.052	65.12
Multiple regression	37.421	0.091	46.43
BP	12.684	0.043	80.92
GA-BP	7.471	0.029	88.39
PSO-BP	3.070	0.018	92.50
SVM	3.467	0.016	93.45
SSA-BP	2.912	0.015	95.59

Table 9: Comparison of the results of different models after processing by the MIV method.

Error representations	Number of input variables	MAPE (%)	RMSE	R^2 (%)
BP	6	13.403	0.042	82.50
GA-BP	5	7.849	0.024	84.62
PSO-BP	5	3.345	0.019	93.36
SVM	5	2.762	0.016	94.93
SSA-BP	5	2.380	0.014	97.31

$$Y = -0.000265 * X2 + 0.043352 * X3 - 0.026143 * X5 + 0.002107 * X7. \tag{18}$$

The last five groups of data were brought into (18), and the calculation results are shown in Table 8. In addition, according to (18), it was not difficult to find that the output variable only had linear relationships with $X2$, $X3$, $X5$, and $X7$. This was basically similar to the analysis results in Section 3.2.

The calculation parameters of BP model were the same as those in Section 3.3. In the GA [20], the learning step was 0.1, the number of genetic iterations was 200, the initial population number was 20, and the classification error was 0.00001. In the PSO [22], inertia weight was 0.6, learning factors $C1$ and $C2$ were 2, initial population number was 20, and maximum iteration number was 200. In the SVM [52], the range of penalty variable was [1, 1000], and the range of width parameter was [0.1, 10]. The related calculation results are shown in Table 8.

From the convergence curves of the GA and the PSO in Figure 4, it is not difficult to find that GA converges in 120–150 generations, while the PSO converges in 80–100 generations. However, the SSA had faster convergence speed than the GA or the PSO.

In this paper, the MIV method was used to screen the input variables of the SSA-BP model, which might affect the calculation results. Therefore, the MIV method was used to screen the input variables of the BP, GA-BP, PSO-BP, and SVM, and the key input variables with relative contribution rate greater than 10% were selected. The calculation results are shown in Table 9.

4.2. Stability Analysis of Different Prediction Models. In addition to the calculation accuracy, the stability of the calculation results of the model is another factor that affects its application and popularization. In this paper, the BP, the GA-BP, the PSO-BP, the SVM, and the SSA-BP were used for repeated calculation 100 times, and the standard deviations of R^2 are shown in Table 10.

It can be seen from the calculation results in Table 10 that the standard deviation of R^2 of SSA-BP model is the smallest (0.001398) and its calculation result is the most stable. The stabilities of the PSO-BP, the GA-BP, and the BP decreased in turn. This showed that the computational stabilities of these metaheuristic algorithms were SSA $(0.001398) >$ PSO $(0.008376) >$ GA (0.023339), which was the same as the previous results [24, 25, 53]. In addition, the standard deviation of R^2 of BP was obviously larger than SSA-BP, PSO-BP, and GA-BP. This indicates that the optimization algorithm is reasonable and effective in improving the BP model. It is worth mentioning that Wu [53] used the SSA to find the optimal parameters of the Least Squares Support Vector Machine (LSSVM) and achieved good results. This further proves the superiority of the SSA, which is a novel metaheuristic optimization algorithm.

4.3. Comparison of the Prediction Results of Different Relative Contribution Rates. Relative contribution rate is an important concept in the MIV model, which is the threshold for selecting key input variables. At present, the selection of this threshold is artificial and subjective [33, 34]. In Section 3, the variables whose relative contribution rates were greater than 10% were selected as the key variables. In order to discuss the rationality of this approach, this paper made a parametric analysis of the relative contribution rate in the MIV. When the relative contribution rate was 5%, 15%, and 20%, the prediction results of the model were calculated and are shown in Table 11.

In this section, the relative contribution rate was analyzed by parameters, and the influence of different input variables on the calculation results was actually analyzed. According to the calculation results in Table 11, when α_i = 10%, the model has the best calculation accuracy and calculation time. This shows that the artificial

Table 10: Stability analysis of different calculation methods.

Calculation method	BP	GA-BP	PSO-BP	SVM	SSA-BP
Number of input variables	6	5	5	5	5
Standard deviation of R^2	0.029487	0.023339	0.008376	0.002843	0.001398

Table 11: Analysis of prediction results under different relative contribution rates.

α_i (%)	Selected input variables	MAPE (%)	RMSE	R^2	Computing time
5	$X7$, $X2$, $X3$, $X4$, $X5$, $X6$	3.047	0.016	95.64	15 min 18 s
10	$X7$, $X2$, $X3$, $X4$, $X5$	2.381	0.014	97.31	13 min 42 s
15	$X7$, $X2$, $X3$	3.515	0.016	92.58	7 min 29 s
20	$X7$, $X2$	5.487	0.018	87.63	5 min 37 s

selection of 10% in most studies using MIV is reasonable. With the increase of the value of α_i, the number of input variables becomes less and less, the calculation error becomes larger and larger, and the calculation time becomes shorter.

When $\alpha_i = 25\%$, only one input variable, $X7$, is selected. At this time, the problem degenerates into studying the mapping relationship between an input variable ($X7$) and an output variable (Y). Therefore, this paper did not discuss the calculation accuracy and time when the value of α_i was larger.

5. Conclusions

It is critically important to rapidly and accurately predict the ticket price to protect the interests of the customer, the private capital investors, and the government. In order to deal with the complexity and nonlinear relationship of the PPP subway system ticket prediction, a new intelligent prediction method is proposed in this paper. The model combines the global convergence of the SSA and the nonlinear analysis ability of a neural network algorithm and improves the accuracy and stability of the neural network training. This study shows that, for Beijing Subway Line 4, Wuhan Metro Line 2, and Chengdu Metro Line 1, the linear relationship between most input variables is not adequate. Among all pairwise correspondences, only three groups of correspondences have significant linear correlation. A nonlinear modeling method should be given priority in the prediction of ticket price for PPP subway system. The MIV method is used to screen the characteristic variables of the ticket price prediction for the PPP subway system, and it is found that the rate of return on investment, total local GDP, number of similar vehicles $X3$, financial subordinate $X4$, and loan interest rate $X5$ can be used as key input variables. Compared with other prediction methods (the price adjustment method based on PPP contract, the traditional BP, the BP improved by the GA, the BP improved by the PSO algorithm, and the SVM), the model proposed in this paper had better prediction accuracy and calculation stability. How to predict the actual fare of subway according to the results of this study is the direction of further research in the future.

Data Availability

The case analysis data used to support the findings of this study are available from the corresponding author upon request.

Conflicts of Interest

The authors declare that there are no conflicts of interest regarding the publication of this paper.

Acknowledgments

This study was supported by the Science and Technology Project of Wuhan Urban and Rural Construction Bureau, China (201943).

References

[1] X. J. Li and P. E. D. Love, "State-of-the-art review of urban rail transit public-private partnerships," *Journal of Infrastructure Systems*, vol. 26, no. 3, Article ID 03120002, 2020.

[2] L. E. Brandão, C. Bastian-Pinto, and L. L. Gomes, "Government supports in public-private partnership contracts: metro line 4 of the sao paulo subway system," *Journal of Infrastructure Systems*, vol. 18, no. 3, pp. 218–225, 2012.

[3] M. De Jong, R. Mu, D. Stead et al., "Introducing public-private partnerships for metropolitan subways in China: what is the evidence?" *Journal of Transport Geography*, vol. 18, no. 2, pp. 301–313, 2010.

[4] H. M. Wang, W. Xiong, G. D. Wu et al., "Public-private partnership in public administration discipline: a literature review," *Public Management Review*, vol. 20, no. 2, pp. 293–316, 2018.

[5] Z. Chang, "Public-private partnerships in China: a case of the Beijing no. 4 Metro line," *Transport Policy*, vol. 30, no. 2013, pp. 153–160, 2013.

[6] S. Sturup, "Swimming or drowning in the depths of partnership," *Australian Journal of Public Administration*, vol. 76, no. 3, pp. 288–300, 2017.

[7] C. Gordon, C. Mulley, N. Stevens et al., "Public-private contracting and incentives for public transport: can anything be learned from the Sydney Metro experience?" *Transport Policy*, vol. 27, no. 2013, pp. 73–84, 2013.

[8] X. J. Li and P. E. D. Love, "Employing land value capture in urban rail transit public private partnerships: retrospective analysis of Delhi's airport metro express," *Research in*

Transportation Business and Management, vol. 32, no. 2019, Article ID 100431, 2019.

[9] R. Cohen and T. Boast, “Governance of public-private partnerships and infrastructure delivery: case of the milan, Italy, metro line *M*4,” *Transportation Research Record*, vol. 2597, no. 1, pp. 37–43, 2016.

[10] K. V. Gestel, T. Willems, K. Verhoest et al., “Public-private partnerships in Flemish schools: a complex governance structure in a complex context,” *Public Money & Management*, vol. 34, no. 5, pp. 363–370, 2014.

[11] A. T. Zhang, “Research on charge pricing of urban rail transit PPP project,” Master thesis, Beijing JiaoTong University, Beijing, China, 2019.

[12] M. D. Bas, J. Ortiz, L. Ballesteros et al., “Evaluation of a multiple linear regression model and SARIMA model in forecasting Be-7 air concentrations,” *Chemosphere*, vol. 177, no. 2017, pp. 326–333, 2017.

[13] K. Nikolopoulos, P. Goodwin, A. Patelis et al., “Forecasting with cue information: a comparison of multiple regression with alternative forecasting approaches,” *European Journal of Operational Research*, vol. 180, no. 1, pp. 354–368, 2007.

[14] C. T. L. Zhou, S. C. Gao, J. H. Wang et al., “Financial time series prediction using a dendritic neuron model,” *Knowledge-Based Systems*, vol. 105, pp. 214–224, 2016.

[15] Y. M. Yang and G. Chen, “Artificial neural network forecasting method in monitoring technique by spectrometric oil analysis,” *Spectroscopy and Spectral Analysis*, vol. 25, no. 8, pp. 1339–1343, 2005.

[16] M. Ray, K. N. Singh, and V. Ramasubramanian, “Integration of wavelet transform with ANN and WNN for time series forecasting: an application to Indian monsoon rainfall,” *National Academy Science Letters-India*, vol. 43, no. 6, pp. 509–513, 2020.

[17] W. P. Cao, X. Z. Wang, Z. Ming et al., “A review on neural networks with random weights,” *Neurocomputing*, vol. 275, no. 2018, pp. 278–287, 2018.

[18] Y. Y. Lv, W. J. Liu, Z. Wang et al., “WSN localization technology based on hybrid GA-PSO-BP algorithm for indoor three-dimensional space,” *Wireless Personal Communications*, vol. 114, no. 1, pp. 167–184, 2020.

[19] C. Chen, N. An, J. Z. Wang et al., “Optimal parameters selection for BP neural network based on particle swarm optimization: a case study of wind speed forecasting,” *Konwledge-Based Systems*, vol. 56, pp. 226–239, 2014.

[20] M. Zou, L. Xue, H. J. Gai et al., “Identification of the shear parameters for lunar regolith based on a GA-BP neural network,” *Journal of Terramechanics*, vol. 89, no. 2020, pp. 21–29, 2020.

[21] H. Qu, K. Xing, and T. Alexander, “An improved genetic algorithm with co-evolutionary strategy for global path planning of multiple mobile robots,” *Neurocomputing*, vol. 120, pp. 509–517, 2013.

[22] R. Nasimi, R. Irani, and R. Ashena, “Optimized scenario for bottomhole pressure prediction in underbalanced drilling based on neural networks coupled with particle swarm optimization,” *Petroleum Science and Technology*, vol. 20, no. 21, pp. 1140–1150, 2012.

[23] G. Shaari, N. Tekbiyik-Ersoy, and M. Dagbasi, “The state of art in particle swarm optimization based unit commitment: a review,” *Process*, vol. 7, no. 10, Article ID 733, 2019.

[24] J. K. Xue and B. Shen, “A novel swarm intelligence optimization approach: sparrow search algorithm,” *Systems Science and Control Engineering*, vol. 8, no. 1, pp. 22–34, 2020.

[25] X. Lv, X. D. Mu, J. Zhang et al., “Chaos sparrow search optimization algorithm,” *Journal of Beijing University of Aeronautics and Astronautics*, 2021.

[26] A. D. Tang, T. Han, D. W. Xu et al., “Path planning method of unmanned aerial vehicle based on chaos sparrow search algorithm,” *Journal of Computer Applications*, vol. 41, no. 7, 2021.

[27] M. Koppen, D. H. Wolpert, and W. G. Macready, “Remarks on a recent paper on the “no free lunch” theorems,” *IEEE Transactions on Evolutionary Computation*, vol. 5, no. 3, pp. 295-296, 2001.

[28] D. H. Li, Q. K. Li, W. C. Wang et al., “Prediction of coal calorific value based on MIV characteristic variable selection and PSO-BP neural network,” *Coal Engineering*, vol. 52, no. 11, pp. 154–160, 2020.

[29] H. Ji, X. Chen, K. Zhang et al., “Construct drawing man-hour forecasting based on GA-BP in chemical equipment design process,” in *Proceedings of the 22nd International Conference on Automation and Computing (ICAC)*, pp. 65–70, Colchester, UK, September 2016.

[30] Y. C. Mao, D. Xiao, J. F. Cheng et al., “Research in magnesite grade classification based on near infrared spectroscopy and ELM algorithm,” *Spectroscopy and Spectral Analysis*, vol. 37, no. 1, pp. 89–94, 2017.

[31] Q. Xu, Z. H. Liu, and S. F. Fang, “Retrieval method for estimating snow depth using hyperspectral data in snowmelt period,” *Spectroscopy and Spectral Analysis*, vol. 33, no. 7, pp. 1927–1931, 2013.

[32] M. Xu, G. M. Zeng, X. Y. Xu et al., “Application of Bayesian regularized BP neural network model for analysis of aquatic ecological data-A case study of chlorophyll-a prediction in Nanzui water area of Dongting lake,” *Journal of Environmental Sciences*, vol. 17, no. 6, pp. 946–952, 2005.

[33] J. Y. Li, C. Men, J. F. Qi et al., “Impact factor analysis, prediction, and mapping of soil corrosion of carbon steel across China based on MIV-BP artificial neural network and GIS,” *Journal of Soils and Sediments*, vol. 20, no. 8, pp. 3204–3216, 2020.

[34] L. Xu, X. L. Zhang, Q. Xiao et al., “Evaluation of pollutant exposure level at bus stop based on MIV-BP neural network,” *Science Technology and Engineering*, vol. 20, no. 30, pp. 12664–12671, 2020.

[35] J. J. Dai, P. F. Shan, and Q. Zhou, “Study on intelligent identification method of coal pillar stability in fully mechanized caving face of thick coal seam,” *Energies*, vol. 13, no. 2, Article ID 305, 2020.

[36] Q. Y. Xing and Y. H. Yuan, “Economic analysis of metro ticket system and political suggestions,” *Urban Mass Transit*, vol. 19, no. 5, pp. 10–14, 2016.

[37] X. Y. Jiang, K. Lu, B. Xia et al., “Identifying significant risks and analyzing risk relationship for construction PPP projects in China using integrated FISM-MICMAC approach,” *Sustainability*, vol. 11, no. 19, Article ID 5209, 2019.

[38] J. Y. Li, F. F. Song, and C. H. Zhao, “Financial compensation strategy of PPP project based on game theory and intelligent optimization,” *Sustainability*, vol. 35, no. 3, pp. 2697–2702, 2018.

[39] Y. L. Wang, J. C. Liu, R. L. Gao et al., “Government subsidies in public-private partnership projects based on altruistic theory,” *International Journal of Strategic Property Management*, vol. 24, no. 3, pp. 153–164, 2020.

[40] B. Wang, S. B. Zhang, X. Q. Wang et al., “The optimal capital structure of PPP projects: based on the real-option method,”

Journal of Management Sciences in China, vol. 22, no. 6, pp. 73–85, 2019.

[41] A. P. C. Chan, P. T. I. Lam, Y. Wen et al., “Cross-sectional analysis of critical risk factors for PPP water projects in China,” *Journal of Infrastructure Systems*, vol. 21, no. 1, Article ID 04014031, 2015.

[42] G. W. Dombi, P. Nandi, J. M. Saxe et al., “Prediction of RIB fracture injury outcome by artificial neutral-network,” *The Journal of Trauma*, vol. 39, no. 5, pp. 915–921, 1995.

[43] H. H. Xu and Y. Deng, “Dependent evidence combination based on Shearman coefficient and Pearson coefficient,” *IEEE Access*, vol. 6, pp. 11634–11640, 2018.

[44] G. Q. Zhang, B. E. Patuwo, and M. Y. Hu, “Forecasting with artificial neural networks: the state of the art,” *International Journal of Forecasting*, vol. 14, no. 1, pp. 35–62, 1998.

[45] X. Zhuang, X. L. Yu, Z. M. Zhao et al., “Application of laser ranging and grey neural network (GNN) for the structure optimization of radio frequency identification (RFID) tags,” *Lasers in Engineering*, vol. 48, no. 1-3, pp. 43–62, 2021.

[46] A. E. Gurel, U. Agbulut, and Y. Bicen, “Assessment of machine learning, time series, response surface methodology and empirical models in prediction of global solar radiation,” *Journal of Cleaner Production*, vol. 277, Article ID 122353, 2020.

[47] Y. B. Sun, L. Chen, B. S. Huang et al., “A rapid identification method for calamine using near-infrared spectroscopy based on multi-reference correlation coefficient method and back propagation artificial neural network,” *Applied Spectroscopy*, vol. 71, no. 7, pp. 1447–1456, 2017.

[48] B. G. Francq and B. Govaerts, “How to regress and predict in a Bland-Altman plot? Review and contribution based on tolerance intervals and correlated-errors-in-variables models,” *Statistics in Medicine*, vol. 35, no. 14, pp. 2328–2358, 2016.

[49] S. C. Gao, Y. Yu, Y. R. Wang et al., “Chaotic local search-based differential evolution algorithms for optimization,” *IEEE Transactions on Systems, Man, and Cybernetics*, vol. 51, no. 6, pp. 3954–3967, 2021.

[50] J. J. Wang and T. Kumbasar, “Parameter optimization of interval type-2 fuzzy neural networks based on PSO and BBBC methods,” *IEEE/CAA Journal of Automatica Sinica*, vol. 6, no. 1, pp. 247–257, 2019.

[51] S. C. Gao, M. C. Zhou, Y. R. Wang et al., “Dendritic neuron model with effective learning algorithms for classification, approximation and prediction,” *IEEE Transactions on Neural Networks and Learning Systems*, vol. 30, no. 2, pp. 601–614, 2019.

[52] X. W. Yang, Q. Z. Yu, L. F. He et al., “The one-against-all partition based binary tree support vector machine algorithms for multi-class classification,” *Neurocomputing*, vol. 113, pp. 1–7, 2013.

[53] H. Wu and J. W. Wang, “A method for prediction of waterlogging economic losses in a subway station project,” *Mathematics*, vol. 9, no. 12, Article ID 1421, 2021.